J|A|C|S
ARTICLES
Published on Web 01/15/2004

β-Cyclodextrin Host−Guest Complexes Probed under Thermodynamic Equilibrium: Thermodynamics and AFM Force Spectroscopy

Tommaso Auletta,[†] Menno R. de Jong,[†] Alart Mulder,[†] Frank C. J. M. van Veggel,[†,§] Jurriaan Huskens,[*,†] David N. Reinhoudt,[*,†] Shan Zou,[‡] Szczepan Zapotoczny,[‡,#] Holger Schönherr,[‡] G. Julius Vancso,[*,‡] and Laurens Kuipers[||]

Contribution from Supramolecular Chemistry and Technology, Materials Science and Technology of Polymers, and Applied Optics, MESA+ Institute for Nanotechnology, University of Twente, P.O. Box 217, 7500 AE Enschede, The Netherlands, and FOM Institute for Atomic and Molecular Physics, Kruislaan 407, 1098 SJ Amsterdam, The Netherlands

Received September 5, 2003; E-mail: j.huskens@utwente.nl; d.n.reinhoudt@utwente.nl; g.j.vancso@utwente.nl

Abstract: The rupture forces of individual host−guest complexes between β-cyclodextrin (β-CD) heptathioether monolayers on Au(111) and several surface-confined guests were measured in aqueous medium by single molecule force spectroscopy using an atomic force microscope. Anilyl, toluidyl, *tert*-butylphenyl, and adamantylthiols (0.2−1%) were immobilized in mixed monolayers with 2-mercaptoethanol on gold-coated AFM tips. For all guests and for all surface coverages, the force−displacement curves measured between the functionalized tips and monolayers of β-CD exhibited single, as well as multiple, pull-off events. The histograms of the pull-off forces showed several maxima at equidistant forces, with force quanta characteristic for each guest of 39 ± 15, 45 ± 15, 89 ± 15, and 102 ± 15 pN, respectively. These force quanta were independent of the loading rate, indicating that, because of the fast complexation/decomplexation kinetics, the rupture forces were probed under thermodynamic equilibrium. The force values followed the same trend as the free binding energy ΔG° measured for model guest compounds in solution or on β-CD monolayers, as determined by microcalorimetry and surface plasmon resonance measurements, respectively. A descriptive model was developed to correlate quantitatively the pull-off force values with the ΔG° of the complexes, based on the evaluation of the energy potential landscape of tip−surface interaction.

Introduction

Short-range interactions determine phenomena such as adhesion, molecular interactions, and molecular recognition. One of the first examples of direct measurements of surface interactions dates back to the surface force apparatus (SFA) developed by Israelachvili and Tabor in the early 1970s.[1] The invention of the atomic force microscope (AFM),[2] well-known for its surface imaging capability, represented a breakthrough in sensitivity for force measurements as well. AFM spring constants k typically vary between 10^{-1} and 10^2 N/m, and cantilever deflections Δz of 0.1 Å can be detected,[3] turning the AFM setup into an extremely sensitive force F measurement apparatus,[4] with a detection limit between 10^{-12} and 10^{-9} N.[5] Forces can be estimated from the measured cantilever deflection according to eq 1.

$$F = k\Delta z \tag{1}$$

So-called "chemical force microscopy" (CFM) combines the resolution available through force microscopy with attractive/repulsive forces taking place between a functionalized probe tip and the sample, allowing compositional mapping of surfaces with different chemical functionalities on the basis of different adhesion properties.[6,7] Furthermore, the possibility to functionalize individually the tip and surface allows investigation of

[†] Supramolecular Chemistry and Technology, University of Twente.
[‡] Materials Science and Technology of Polymers, University of Twente.
[||] Applied Optics, University of Twente, and FOM Institute for Atomic and Molecular Physics.
[§] Present address: University of Victoria, Department of Chemistry, P.O. Box 3065 STN CSC Victoria, BC V8W 3V6, Canada.
[#] Present address: Jagiellonian University, Faculty of Chemistry, Ingardena 3, 30-060 Krakow, Poland.

(1) Israelachvili, J. N.; Tabor, D. *Proc. R. Soc. London, Ser. A* **1972**, *331*, 19−38.
(2) Binnig, G.; Quate, C. F.; Gerber, C. *Phys. Rev. Lett.* **1986**, *56*, 930−933.
(3) Putman, C. A. J.; DeGrooth, B. D.; Van Hulst, N. F.; Greve, J. *J. Appl. Phys.* **1992**, *72*, 6−12.
(4) (a) Evans, E.; Ritchie, K.; Merkel, R. *Biophys. J.* **1995**, *68*, 2580−2587. (b) Kuo, S. C.; Sheetz, M. P. *Science* **1993**, *260*, 232−234 and references cited herein.
(5) Other techniques utilize magnetic beads, optical tweezers, microneedles, and biomembrane force probes with typical force ranges of 0.1−100 pN, 0.1−150 pN, >0.1 pN, and 0.5−1000 pN, respectively (see, for example, Clausen-Schaumann, H.; Seitz, M.; Krautbauer, R.; Gaub H. E. *Curr. Opin. Chem. Biol.* **2000**, *4*, 524−530).
(6) (a) Frisbie, C. D.; Rozsnyai, L. F.; Noy, A.; Wrighton, M. S.; Lieber, C. M. *Science* **1994**, *265*, 2071−2074. (b) Noy, A.; Vezenov, D. V.; Lieber, C. M. *Annu. Rev. Mater. Sci.* **1997**, *27*, 381−421.
(7) For sub-50-nm resolution mapping of functional group distributions in surface-modified polymers, see: (a) Schönherr, H.; Hruska, Z.; Vancso, G. J. *Macromolecules* **2000**, *33*, 4532−4537. (b) Schönherr, H.; van Os, M. T.; Hruska, Z.; Kurdi, J.; Förch, R.; Arefi-Khonsari, F.; Knoll, W.; Vancso G. J. *J. Chem. Soc., Chem. Commun.* **2000**, 1303−1304. (c) Schönherr, H.; van Os, M. T.; Förch, R.; Timmons, R. B.; Knoll, W.; Vancso G. J. *Chem. Mater.* **2000**, *12*, 3689−3694.

specific combinations of molecular pairs.[8] A wide variety of examples has been reported, ranging from biological systems,[9−11] rupture of covalent bonds,[12] and chiral discrimination[13] to rupture forces of individual charge-transfer complexes[14] and cation complexation.[15]

Several studies exist in which the dissociation of molecular pairs has been theoretically modeled.[16−19] Furthermore, several attempts to correlate the force values measured in single molecule force spectroscopy with thermodynamic parameters of molecular recognition or surface adhesion have been reported.[16a,c] However, studies on molecular unbinding events and host−guest (HG) complex rupture forces under thermodynamic equilibrium conditions remain scarce,[20,21] while for far-from-equilibrium systems the unbinding forces are, depending on the regime, highly loading rate-dependent,[22] as demonstrated by Evans and co-workers.[23]

Previous studies in our groups have been carried out on the complexation behavior of ferrocene moieties immobilized on AFM tips and heptathioether β-cyclodextrin (β-CD) self-assembled monolayers (SAMs) on Au(111).[24,25] β-CD is a cyclic oligosaccharide consisting of seven glucose units linked via α-1−4 glycosidic bonds that is able to form inclusion complexes with a variety of neutral and charged organic molecules in aqueous solutions, mainly via hydrophobic interactions.[26,27] Such HG systems are characterized by fast complexation/decomplexation kinetics, and thus, the guest moieties decomplex and rebind spontaneously many times during the recording of an AFM force−distance curve as long as the tip stays in close proximity to the β-CD SAM. Thus, thermodynamic equilibrium, as defined for our systems including the cantilever, is reached for each data point of a force−distance curve.

The statistical analysis of the pull-off data for the ferrocene−β-CD system showed a periodic distribution of forces.[24,25] In accordance with the long timescale of the AFM pull-off experiments relative to the complexation kinetics and the thermodynamic equilibrium situation that should result from it, the force quantum (55 ± 10 pN) attributed to the single HG complex rupture force was independent of the number of available guests, the loading rate, and the length of the spacer between the guest and the surface.[24,25]

The work presented in this article is a systematic study of single HG complex rupture forces between β-CD SAMs and several guest molecules confined onto the surface of gold-coated AFM tips by adsorption in mixed SAMs. Four different thiol-modified guests have been used to vary the HG interaction strength. The complexation constants for model guest compounds in solution or on β-CD SAMs have been determined by isothermal titration calorimetry (ITC) and surface plasmon resonance (SPR) measurements. The notion of thermodynamic equilibrium allows us to correlate quantitatively the measured pull-off force values with the $\Delta G°$ of the complexes using a newly developed quantitative model that is based on the evaluation of the energy potential landscape of the tip−surface interactions.

Results and Discussion

We have previously reported that the force quantum of 55 ± 10 pN, attributed to the rupture of a single inclusion complex of β-CD heptathioether **1** (Chart 1A) on Au(111) and the ferrocenylalkanethiol **4** (Chart 1B) immobilized on an AFM tip, arises from specific HG interactions, as was proven by systematically leaving out the host or guest from the system and by competition experiments with a guest in solution.[24] This quantum does not depend on spacer length, loading rate, and guest concentration on the tip.[24,25] Four different thiol-modified guests, **2**, **3**, **5**, and **6** (Chart 1B), were synthesized to investigate how changes in the HG motif would affect the rupture force.

The synthesis of adsorbate **1** and preparation of SAMs on gold surfaces have been described elsewhere.[28] Compounds **2**, **3**, **5**, and **6** were synthesized by reacting suitable amines with 5-bromopentanoic acid and followed by substitution of the bromide for thioacetate and subsequent deprotection. Mixed SAMs of 0.2% or 1% of these guest thiols with 2-mercaptoethanol on gold substrates and on gold-modified AFM tips were prepared from 1 mM (total thiol concentration) solutions in ethanol for 16 h at room temperature.

Figure 1 shows a schematic representation of the supramolecular single molecule force spectroscopy experiment with an arbitrary surface-confined guest. Force−displacement curves for guest surface coverages on the tip obtained from 0.2% and 1% solutions show single, as well as characteristic multiple, pull-off events, as shown for **6** in Figure 2A.

(8) For recent reviews, see: (a) Hugel, T.; Seitz, M. *Macromol. Rapid Commun.* **2001**, *22*, 989−1016. (b) Zlatanova, J.; Lindsay, S. M.; Leuba, S. H. *Prog. Biophys. Mol. Biol.* **2000**, *74*, 37−61. (c) Janshoff, A.; Neitzert, M.; Oberdörfer, Y.; Fuchs, H. *Angew. Chem., Int. Ed.* **2000**, *39*, 3212−3237. (d) Samorì, B. *Chem.−Eur. J.* **2000**, *6*, 4249−4255.
(9) (a) Florin, E.-L.; Moy, V. T.; Gaub, H. E. *Science* **1994**, *264*, 415−417. (b) Moy, V. T.; Florin, E.-L.; Gaub, H. E. *Science* **1994**, *266*, 257−259.
(10) Lee, G. U.; Chrisey, L. A.; Colton, R. J. *Science* **1994**, *266*, 771−773.
(11) Ros, R.; Schwesinger, F.; Anselmetti, D.; Kubon, M.; Schäfer, R.; Plückthun, A.; Tiefenauer, L. *Proc. Natl. Acad. Sci. U.S.A.* **1998**, *95*, 7402−7405.
(12) Grandbois, M.; Beyer, M.; Rief, M.; Clausen-Schaumann, H.; Gaub, H. E. *Science* **1999**, *283*, 1727−1730.
(13) McKendry, R.; Theoclitou, M.-E.; Rayment, T.; Abell, C. *Nature* **1998**, *391*, 566−568.
(14) Skulason, H.; Frisbie, C. D. *J. Am. Chem. Soc.* **2002**, *124*, 15125−15133.
(15) Kado, S.; Kimura, K *J. Am. Chem. Soc.* **2003**, *125*, 4560−4564.
(16) (a) Grubmuller, H.; Heymann, B.; Tavan, P. *Science* **1996**, *271*, 997−999. (b) Heymann, B.; Grubmuller, H. *Phys. Rev. Lett.* **2000**, *84*, 6126−6129. (c) Heymann, B.; Grubmuller, H. *Biophys. J.* **2001**, *81*, 1295−1313. (d) Rief, M.; Grubmuller, H. *ChemPhysChem* **2002**, *3*, 255−261.
(17) Bell, G. I. *Science* **1978**, *200*, 618−627.
(18) (a) Hummer, G.; Szabo, A. *Proc. Natl. Acad. Sci. U.S.A.* **2001**, *98*, 3658−3661. (b) Hummer, G.; Szabo, A. *Biophys. J.* **2003**, *85*, 5−15.
(19) (a) Seifert, U. *Phys. Rev. Lett.* **2000**, *84*, 2750−2753. (b) Seifert, U. *Europhys. Lett.* **2002**, *58*, 792−798.
(20) (a) Rief, M.; Clausen-Schaumann, H.; Gaub, H. E. *Nat. Struct. Biol.* **1999**, *6*, 346−349. (b) Essevaz-Roulez, B.; Bockelmann, U.; Heslot, F. *Proc. Natl. Acad. Sci. U.S.A.* **1997**, *94*, 11935−11940.
(21) Tromas, C.; Rojo, J.; de la Fuente, J. M.; Barrientos, A. G.; García, R.; Penadés, S. *Angew. Chem., Int. Ed.* **2001**, *40*, 3052−3055.
(22) (a) Rief, M.; Gautel, M.; Osterhelt, F.; Fernandez, J. M.; Gaub, H. E. *Science* **1997**, *276*, 1109−1112. (b) Fritz, J.; Katopodis, A. G.; Kolbinger, F.; Anselmetti, D. *Proc. Natl. Acad. Sci. U.S.A.* **1998**, *95*, 12283−12288. (c) Marszalek, P. E.; Lu, H.; Li, H.; Carrion-Vazquez, M.; Oberhauser, A. F. *Nature* **1999**, *402*, 100−103. (d) Strunz, T.; Oroszlan, K.; Shafer, R.; Güntherodt, H.-J. *Proc. Natl. Acad. Sci. U.S.A.* **1999**, *96*, 11277−11282. (e) Evans E.; Ludwig, F. *J. Phys.: Condens. Matter* **2000**, *12*, 315−320. (f) Baumgartner, W.; Hinterdorfer, P.; Ness, W.; Raab, A.; Vestweber, D. *Proc. Natl. Acad. Sci. U.S.A.* **2000**, *97*, 4005−4010. (g) Lee, I.; Marchant. R. E. *Surf. Sci.* **2001**, *491*, 433−443.
(23) (a) Evans, E.; Ritchie, K. *Biophys. J.* **1997**, *72*, 1541−1555. (b) Merkel, R.; Nassoy, P.; Leung, A.; Ritchie, K.; Evans, E. *Nature* **1999**, *397*, 50−53.
(24) Schönherr, H.; Beulen, M. W. J.; Bügler, J.; Huskens, J.; van Veggel, F. C. J. M.; Reinhoudt, D. N.; Vancso, G. J. *J. Am. Chem. Soc.* **2000**, *122*, 4963−4967.
(25) Zapotoczny, S.; Auletta, T.; De Jong, M. R.; Schönherr, H.; Huskens, J.; van Veggel, F. C. J. M.; Reinhoudt, D. N.; Vancso, G. J. *Langmuir* **2002**, *18*, 6988−6994.
(26) (a) Wenz, G. *Angew. Chem., Int. Ed. Engl.* **1994**, *33*, 803−822. (b) *Chem. Rev.* **1998**, *98*, 1741−2076. (c) Szejtli, J. *Comprehensive Supramolecular Chemistry*; Pergamon Press: Oxford, 1996; Vol. 3.
(27) Rekharsky, M. V.; Inoue, Y. *Chem. Rev.* **1998**, *98*, 1875−1917.
(28) De Jong, M. R.; Huskens, J.; Reinhoudt, D. N. *Chem.−Eur. J.* **2001**, *7*, 4164−4170.

Chart 1. Chemical Structure of β-CD Adsorbate **1** (A), Guest Molecules **2**−**6** Immobilized at AFM Tips (B), and Model Guests **7**−**11** for HG Binding in Solution and at SAMs of **1** (C)

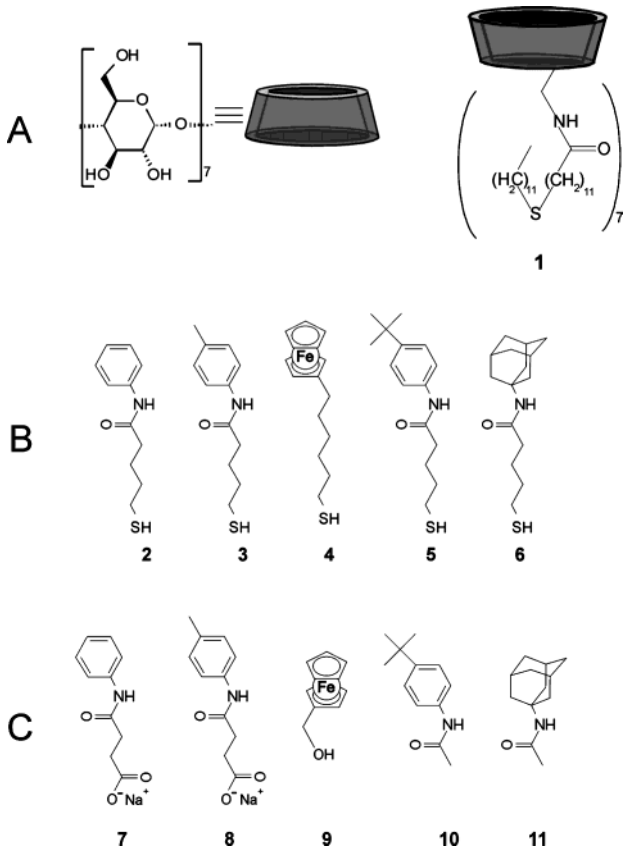

The measured cantilever deflections corresponding to the pull-off events were translated into force using the independently determined AFM cantilever spring constants, which were in the range 0.05−0.12 N/m. All pull-off forces determined from individually resolved events were plotted in histograms.[29] Fast Fourier transform (FFT) smoothing[30] of the force histograms for tips functionalized with **2**, **3**, **5**, or **6** shows a periodic distribution of forces, regardless of the bin size, with force quanta of 39 ± 15, 45 ± 15, 89 ± 15, 102 ± 15 pN, respectively (Figure 3).[31] The loading rate was varied over several orders of magnitude for tips covered with mixed SAMs of 2-mercaptoethanol containing 1% of guest. In agreement with previous reports,[24,25] the quantized force was unaffected by the loading rate for any of the guests, even for the strongest binding guest **6** (Figure 2B).

ITC and SPR measurements were employed to evaluate the thermodynamics of complex formation in solution and on surfaces, respectively, between compounds **7**−**11** (Chart 1C), which function as model systems for compounds **2**−**6**, respectively, and β-CD hosts. The solution-binding parameters for compounds **9**−**11** with native β-CD in solution, determined by

(29) There appear to be some differences in the probabilities for observing multiple force quanta, for example, for **3** (Figure 3B), which may arise from: (i) differences in solubilities and adsorptivities of the guest thiols leading to different guest−mercaptoethanol ratios on the tip than present in solution, (ii) different degrees of clustering of guests on the tip, rendering some guest molecules inaccessible for binding, and (iii) variations in tip geometry and tip−surface contact areas.
(30) The data in the histograms were treated as described in refs 24 and 25.
(31) Noise levels were ∼15 pN. Plots of peak position from the histograms versus peak number yielded straight lines, with the force quantum as the slope (see also ref 25).

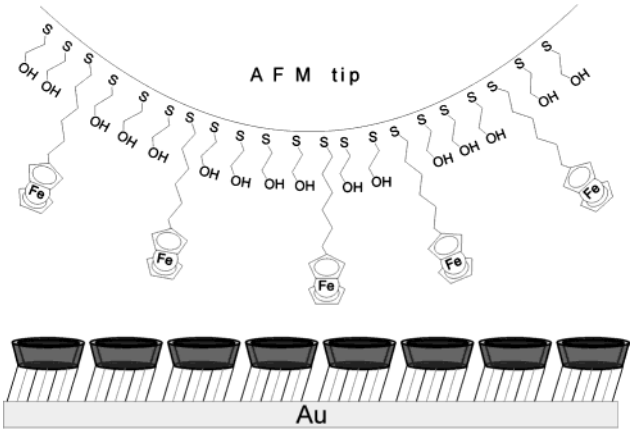

Figure 1. Schematic representation (not to scale) of AFM-based single molecule force spectroscopy of ferrocene guest **4** immobilized in a hydroxyl-terminated SAM on an AFM tip and a SAM of **1** on Au(111).

ITC, have been reported previously.[28] The same approach was applied to determine the thermodynamics of the HG complexes of **7** and **8**. SPR measurements were employed to determine the complexation constants on SAMs of **1** only for compounds **9**−**11**, since poor solubility and weak interactions for compounds **7** and **8** prevented reliable measurements. The experimental data for compounds **9**−**11**, obtained by means of the two independent techniques, show an excellent agreement, as seen in Table 1. These results are also in agreement with the observation reported earlier[28] that small guest molecules, which fit into the CD cavity, apparently do not feel the presence of the alkyl chains of **1**, leading to identical binding constants in solution and at β-CD SAMs. This notion therefore allowed us to extrapolate the ITC results to the binding parameters on surfaces of compounds **7** and **8**.

Table 1 summarizes the single HG complex rupture force values determined for the interaction of SAMs of **1** with SAMs of adsorbates **2**−**6** and the thermodynamic parameters for HG complexes of β-CD with compounds **7**−**11**.[25] The data clearly show a correlation of $\Delta G°$ and unbinding forces. This result, together with the loading rate independence of the force values, strongly supports our view of a process occurring under thermodynamic equilibrium. Therefore, these results open the possibility to investigate the relation between rupture forces and thermodynamic quantities, such as the Gibbs free energy of binding, $\Delta G°$.

Expanding on the approach proposed by Hansma and coworkers for measuring interaction potentials,[32] Willemsen et al. demonstrated that the total potential can be derived from the probability distribution of the tip position by monitoring the Brownian movement of an AFM tip in a potential well.[33] The total potential consists of the sum of the harmonic cantilever potential and the tip−surface interaction potential.

Here we describe a model to correlate $\Delta G°$ and the dissociation force, $F_{\text{pull-off}}$, for an individual HG pair. It requires: (i) the generalization and formalization of the tip−surface interaction, which is governed by the HG interaction and is approximated here using a Lennard-Jones potential (LJP) description, the well depth of which is the guest-specific parameter,

(32) Cleveland, J. P.; Schäffer, T. E.; Hansma, P. K. *Phys. Rev. B* **1995**, *52*, R8692−R8695.
(33) Willemsen, O. H.; Kuipers, L.; Van der Werf, K. O.; De Grooth, B.; Greve, J. *Langmuir* **2000**, *16*, 4339−4347.

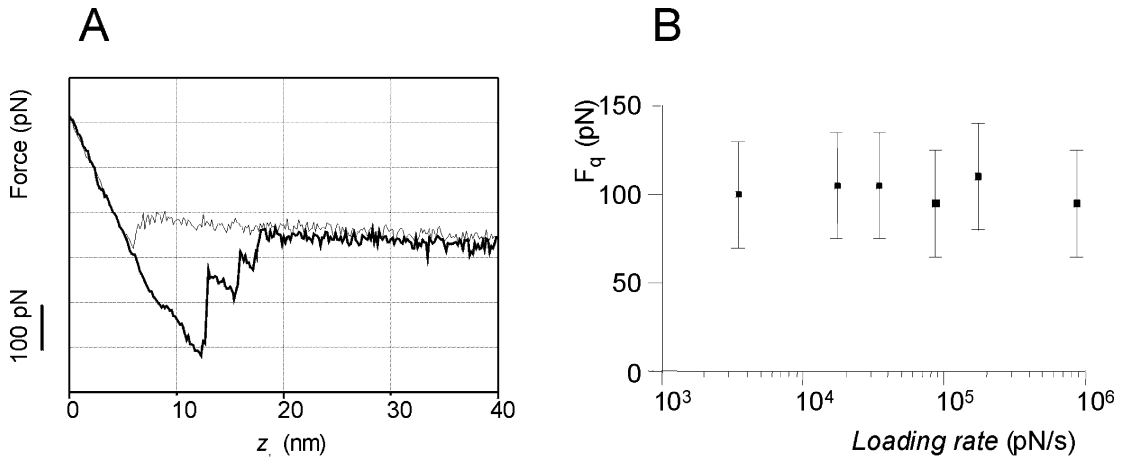

Figure 2. Representative force−distance curve for the interaction of a tip covered with a mixed SAM of 1% of **6** and 2-mercaptoethanol with a SAM of **1** (A) and loading rate dependence for the same system (B).

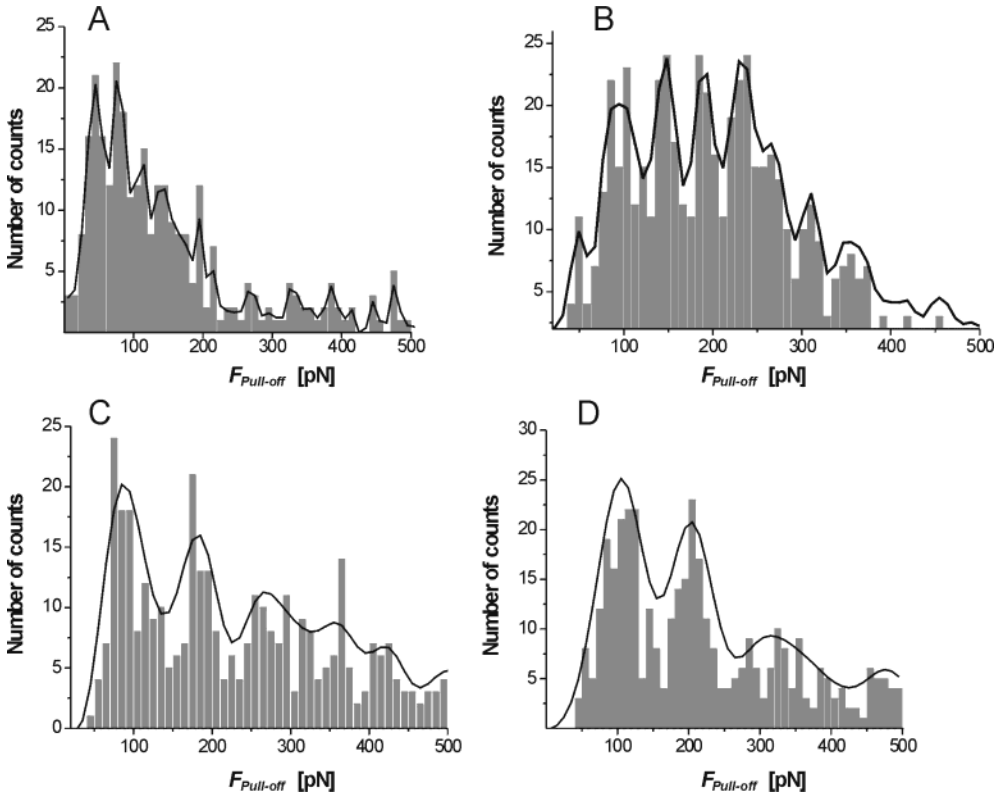

Figure 3. Histograms for the interaction of tips coated with 1% of **2** (A), 1% of **3** (B), 1% of **5** (C), and 1% of **6** (D) and 2-mercaptoethanol with SAMs of **1** (bin size 8 pN). The solid lines represent the FFT-smoothed histograms.

Table 1. Force Values, $F_{pull-off}$, for Guests **2**−**6** Measured by Force Spectroscopy, Thermodynamic Data at SAMs of **1** for Model Compounds **9**−**11** Measured by SPR, and Solution Data for Model Compounds **7**−**11** with Native β-CD Measured by ITC

	AFM		SPR	ITC		
guest	$F_{pull-off}$ pN	model guest	$\Delta G°$ kcal mol^{-1}	$\Delta G°$ kcal mol^{-1}	$\Delta H°$ kcal mol^{-1}	$T\Delta S°$ [d] kcal mol^{-1}
2	39 ± 15	**7**	*a*	−2.3	−2.3	0.0
3	45 ± 15	**8**	*a*	−3.0	−2.7	0.3
4	55 ± 10[b]	**9**	−5.4[c]	−5.4[c]	−6.1[c]	−0.7[c]
5	89 ± 15	**10**	−6.0[c]	−6.1[c]	−5.2[c]	0.9[c]
6	102 ± 15	**11**	−6.5[c]	−6.6[c]	−5.9[c]	0.7[c]

[a] Low solubility and weak interactions with the CD SAM do not allow accurate measurements of the thermodynamic parameters for this guest. [b] From ref 25. [c] From ref 28. [d] T = 298 K.

(ii) a space integration of the HG potential energy to correlate the LJP well depth to the macroscopic stability constant K and thus to $\Delta G°$, (iii) a total potential energy description and a probability distribution for the tip being or not being in contact

with the sample surface to correlate the LJP well depth to the (maximum) cantilever deflection at which the pull-off event occurs and thus to $F_{pull-off}$, and (iv) a combination of these correlations to give a theoretical prediction of $F_{pull-off}$ as a function of $\Delta G°$.

The model described below applies in principle only to the interactions existing between one single guest on the tip and one β-CD cavity on the surface. Multiple, simultaneous pull-off events were not taken into consideration. In an earlier study,[25] we showed that the multiple binding events corresponded to multiple forces of a single event and that the fraction of single-rupture events (with the same force quanta) increased upon lowering the amount of guest on the tip. Therefore, we assumed that an understanding of a single pull-off event of a single HG pair sufficed to describe the systems at hand.

In our system, a potential energy description was used to model the HG system. Molecular dynamics (MD) calculations were employed to describe the potential energy of the HG complex for a linear dissociation pathway, i.e., the guest, in this case ferrocene, was pulled out of the cavity, and driven by the tip along the symmetry axis of the β-CD cavity.

The interactions of a β-CD cavity with a guest can be described by a potential energy well, the shape of which is approximated by an LJP (eq 2).

$$U_{LJP}(z) = 4\epsilon\left(\left(\frac{s}{z+z_0}\right)^{12} - \left(\frac{s}{z+z_0}\right)^{6}\right) \qquad (2)$$

Here z represented the distance from the LJP minimum along the dissociation pathway, z_0 was an offset parameter with a value of $s\sqrt[6]{2}$ (ensuring that the well minimum occurred at $z = 0$: $U_{LJP}(0) = -\epsilon$ and $dU_{LJP}/dz = 0$), ϵ was the well depth, and s determined the width of the well. The MD simulation data for ferrocene (as a model for guests **4** and **9**) were fitted to the LJP in a least-squares optimization routine (see Supporting Information), while varying ϵ, s, and z_0. The width of the well (s = 7.78 Å), which corresponded well to the depth of the cyclodextrin cavity (8 Å), was the only parameter obtained from the MD simulations that was used in the theoretical description described below. The z_0 parameter was an offset parameter only, and the well depth ϵ was varied for all guests depending on K, as was obtained by a space integration of the potential energy as described below. For all other guest motifs employed in this study, we assumed the same well shape, i.e., s was kept constant, while ϵ was varied to account for changes in $\Delta G°$.

A space integration of $U_{LJP}(z)$ allowed us to correlate the depth of the well ϵ associated with each HG complex to the corresponding $\Delta G°$ value via the complexation constant K. In a first attempt, a relationship between the HG equilibrium constant K and the potential energy was applied to simulate hydrophobic interactions and, thus, molecular recognition.[34] This calculation was based on the space integration of U_{LJP} with a radial dependence according to eq 3, where N_{av} was Avogadro's number. In our case, the space integration over $z \geq 0$ represented a hemisphere above the β-CD cavity, while $z \leq 0$ represented the cavity interior (repulsive interactions of LJP). This integration may not describe the 3D interaction dependence correctly since, as stated above, the pull-off trajectory of the guest out of the cavity can better be assumed to be linear. Therefore, in an alternative second integration approach, the sampled volume was restricted to a cylinder defined by the area available for in-plane movement of the guest in the cavity ($A_{CD} = \pi r^2$ with r = 2 Å) and the linear trajectory perpendicular to this area along which the guest dissociated (eq 4).

$$K = 2\pi N_{av}\int_{-}^{+\infty} z^2 \exp[-U_{LJP}(z)/RT]\, dz \qquad (3)$$

$$K = N_{av}A_{CD}\int_{-\infty}^{+\infty} \exp[-U_{LJP}(z)/RT]\, dz \qquad (4)$$

Employing $\Delta G° = -RT \ln K$ led to the following linear relationships: $-\Delta G° = 0.93\epsilon - 4.15$ and $-\Delta G° = 0.97\epsilon - 2.79$ for the spherical and the cylindrical integrations, respectively, with $-\Delta G°$ and ϵ in kcal mol^{-1}. The $\Delta G°$ values of the HG systems studied here varied between −2.3 and −6.4 kcal mol^{-1}, as determined from ITC and SPR measurements, and thus ϵ ranged from −6.6 to −11.4 kcal mol^{-1} or from −5.3 to −9.5 kcal mol^{-1}, respectively.

To assess the sensitivity of the geometrical parameter A_{CD} on the integration step, the relationship between $-\Delta G°$ and ϵ was derived for two other different values of r (r = 1 Å and r = 4 Å). From the data it can be observed that changes in the geometrical parameter A_{CD} did not affect the slope of the curve of $-\Delta G°$ vs ϵ but only modified the intercept (for r = 1 Å: $-\Delta G = 0.97\epsilon - 3.59$, and for r = 4 Å: $-\Delta G = 0.97\epsilon - 1.99$). Therefore, as an approximation, the value of r = 2 Å was assumed to hold for all the guests.

To combine tip and HG potentials, the LJP needed to be modified to include the presence of the alkyl spacer with length L between the guest moiety and the AFM tip. The alkyl chain was treated as an infinitely flexible linker until the maximum elongation was reached, although it could not be stretched beyond its fully elongated conformation. These considerations resulted in a total potential energy of the complex $U_{complex}(z) = U_{LJP}(z + L)$ for $z \leq -L$, $U_{complex}(z) = -\epsilon$ for $-L \leq z \leq 0$, and $U_{complex}(z) = U_{LJP}(z)$ for $z \geq 0$.

The cantilever potential U_{tip} was described by a harmonic potential (eq 5)

$$U_{tip}(z) = (1/2)k(z - z_1)^2 \qquad (5)$$

where $\Delta z = z - z_1$ was the cantilever deflection and z_1 represented the tip position, i.e., the position of the minimum of the cantilever parabola potential, which was controlled by the piezo movement.

The total potential energy of the system could now be derived as the sum of the modified LJP describing the HG complex and the harmonic potential describing the cantilever potential (eq 6).

$$U_{tot}(z) = U_{complex}(z) + U_{tip}(z) \qquad (6)$$

Changes in the tip position were reflected in the total potential energy curve. Initially, when the piezo was not yet moved and no cantilever deflection occurred ($\Delta z = 0$, $-L < z_1 < 0$), the positions of the minima of $U_{complex}$ and U_{tip} coincided, and only one minimum for U_{tot} was observed (Figure 4A, $z_1 = 0$). Retraction of the piezo (in our setup, z_1 was recorded in steps of typically 2 Å)[35] was translated into a cantilever deflection

(34) (a) Pangali, C. S.; Rao, M.; Berne, B. J. *J. Chem. Phys.* **1979**, *71*, 2975−2981. (b) Jorgensen, W. L. *Acc. Chem. Res.* **1989**, *22*, 184−189.

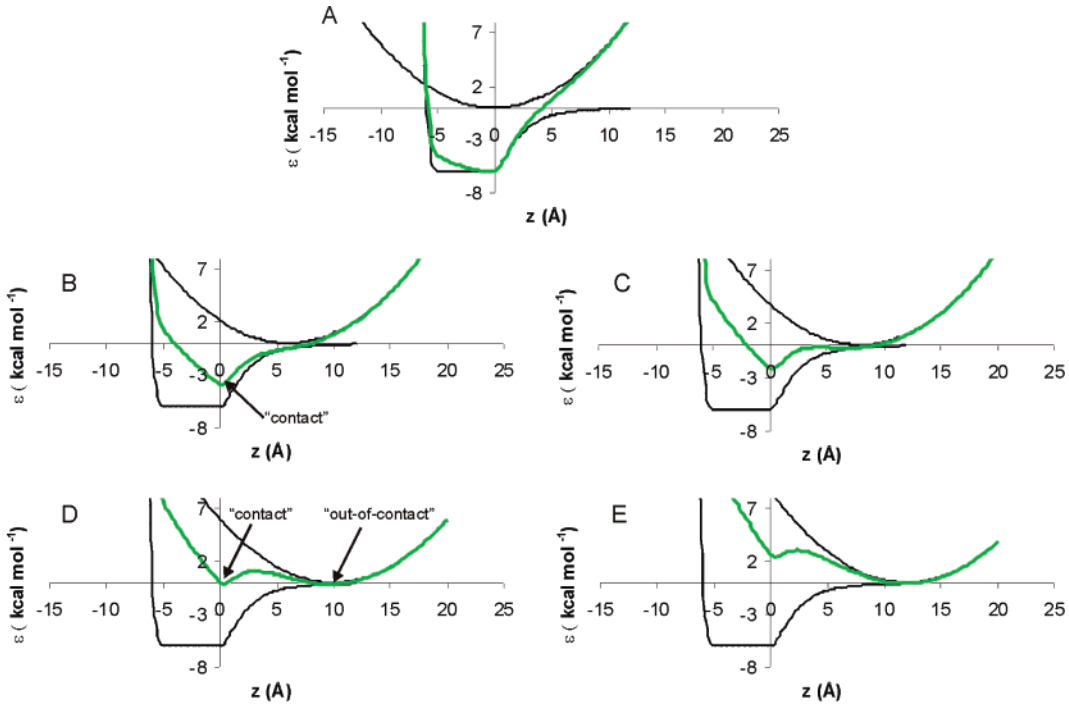

Figure 4. Total energy description: U_{tip} (parabola), $U_{complex}$ (black line), and U_{tot} (gray line). The tip position z_1 from A to E is 0, 6, 8, 10, and 12 Å, respectively ($\epsilon = 6$ kcal mol^{-1}).

($\Delta z > 0$) with a shift of the parabola potential minimum z_1 to the right, thus raising the minimum observed at $z = 0$ for the total potential energy curve (Figure 4B). Up to a certain point, only one minimum existed, called "contact", in which the tip stayed in contact with the sample, while the HG complex may rapidly dissociate and reassociate. It can also be seen in Figure 4 that this "contact" minimum stayed at the same position, i.e., at $z = 0$, because of the larger stiffness of the complex,[36] so that the observed deflection Δz was equal to z_1. Near the point where a pull-off event takes place, a second minimum, called "out-of-contact", appeared and quickly became the predominant one (Figure 4D). In this minimum, the tip was not in contact with the surface, and the HG complex was dissociated. In Figure 4B−E, the change in tip position z_1 was simulated by four sequential energy potential curves, with $z_1 = 6$, 8, 10, and 12 Å, respectively, corresponding to consecutive data points in a (simulated) pull-off experiment. The plots show the corresponding changes in U_{tot} and describe the transition from the "contact" to the "out-of-contact" state as the most energetically favorable situation.

According to Boltzmann statistics, the relative probability $p(z)$ for the system to exist in situation (z, $U_{tot}(z)$) is given by eq 7.

$$p(z) = \exp[-U_{tot}(z)/RT] \tag{7}$$

In the case when two minima are present, separated by a barrier which has a maximum at $z = z_{bar}$, the probability for the system to be in the "contact" state, $p_{contact}$, is given by eq 8, which is a function of z_1.

$$p_{contact} = \frac{\int_{-\infty}^{z_{bar}} p(z)\,dz}{\int_{-\infty}^{\infty} p(z)\,dz} = \frac{\int_{-\infty}^{z_{bar}} \exp[-U_{tot}(z)/RT]\,dz}{\int_{-\infty}^{\infty} \exp[-U_{tot}(z)/RT]\,dz} \tag{8}$$

Obviously, $p_{out-of-contact}$ could be obtained from integrating $p(z)$ for $z > z_{bar}$, and $p_{contact} + p_{out-of-contact} = 1$.

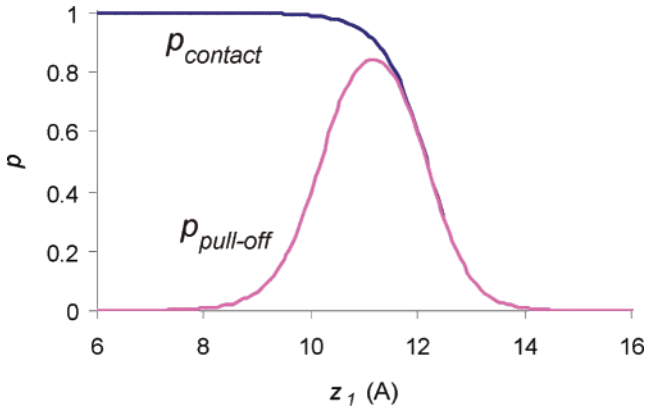

Figure 5. Plot of $p_{contact}$ (black line) and $p_{pull-off}$ (gray line) as a function of z_1 ($\epsilon = 10$ kcal mol^{-1}).

Figure 5 shows $p_{contact}$ as a function of z_1 for $\epsilon = 10$ kcal mol^{-1}, as obtained after numerical integration.[37] Here it is seen that $p_{contact}$ dropped from 1 to 0 in about 4 Å, i.e., typically within only two data points. The specific z_1 value at which this occurred obviously depended on ϵ, but the shape of the curve hardly changed. A macroscopic pull-off event thus corresponded to one data point being in the "contact" state, while for the next data point the "out-of-contact" state was observed. Thus, the probability $p_{pull-off}$ to observe such a pull-off event can be defined as in eq 9.

(35) The measured pull-off forces did not vary for nominal spacings of the data points between 1 and 10 Å.
(36) The stiffness of the complex as a function of ϵ is described by $k_{complex} = 23.81\epsilon$ [pN Å^{-1}], with ϵ in kcal mol^{-1} (see the Supporting Information).
(37) Alternatively, a semianalytical expression can be derived relating $p_{contact}/p_{out-of-contact}$ to the energy difference between the two minima, eliminating the need for the numerical integration (see the Supporting Information). Here, the interaction potential at the well of the "contact" minimum is also fitted to a harmonic potential. This analysis shows that the probability distribution depends only marginally on the "stiffness" of the complex (which governs the harmonic interaction potential and which is directly related to the well width s).

$$p_{\text{pull-off}}(z_1) = p_{\text{contact}}(z_1) \times p_{\text{out-of-contact}}(z_1 + 2) = p_{\text{contact}}(z_1) \times (1 - p_{\text{contact}}(z_1 + 2)) \quad (9)$$

The dependence of $p_{\text{pull-off}}$ with z_1 is shown in Figure 5 as well. Again, the steep dependence of $p_{\text{pull-off}}$ with z_1 ensured that the pull-off event occurred at a specific data point and that no switching back and forth between the "contact" and the "out-of-contact" states would be observed in the experimental setup used here, unless one were to detect data points for relatively long periods of time at all z_1 of a pull-off experiment,[38] as was done and observed recently for another system.[33] The curve also shows that z_1, for which the pull-off was observed, had a certain distribution (approximately ±1.5 Å) for an identical HG complex probed under identical conditions, corresponding to a force variability of ±10 pN.

Once the maximum pull-off probability was determined, the corresponding tip deflection Δz_{max} was converted into the force exerted by the cantilever according to eq 10, thus determining the pull-off force value.

$$F_{\text{pull-off}} = k_{\text{tip}} \Delta z_{\text{max}} \quad (10)$$

From the above-described model, it was possible to derive the dependence of $p_{\text{pull-off}}$ and thus the dependence of the pull-off force with ϵ. This dependence appeared to be a square root dependence ($F = 31.25 \times \sqrt{\epsilon - 1.75}$; see Figure 6A).

The relationship between ϵ and $-\Delta G°$ described above allowed us to extend the correlation between energy and force to the thermodynamics of the HG complex. Figure 6B reports the derived dependence of pull-off force vs $-\Delta G°$ for the spherical and cylindrical integration approaches, $F = 32.60 \times \sqrt{-\Delta G + 2.39}$ and $F = 31.76 \times \sqrt{-\Delta G + 1.03}$, respectively (with $-\Delta G°$ in kcal mol^{-1} and F in pN). The experimental values for the five HG complexes investigated are shown as well.

The theoretically derived square root dependence of $F_{\text{pull-off}}$ with $-\Delta G°$ can intuitively be understood from the fact that a deeper well ϵ (and thus a linear change in $\Delta G°$) can be compensated by a square root change in z_1 and thus in force, since the potential energy of the cantilever depends quadratically on deflection.

In Figure 6B, it can be seen that the fit to the experimental data improved significantly upon changing the integration volume from a spherical to a cylindrical type (the average rms difference between the predicted and experimental force values amounted to 26 pN for the former and 18 pN for the latter), with changes in both the slope and intercept with the y axis of the two curves and lower energy values for the cylindrical integration. These results thus suggested that the assumption of a linear dissociation pathway for a guest linked to, and thus driven by, the AFM tip described more accurately the events occurring at the molecular level. It must be noted, however, that although the fit improved, the change in the integration volume did not severely affect the corresponding force value. In Figure 6B, it can be observed as well that both curves possessed an intercept with the x axis at positive $\Delta G°$ values. The model thus predicted a measurable pull-off force for a molecular species that interacted so weakly with one cyclodextrin cavity that the equilibrium complexation constant K was less than 1.0. For the ferrocene system, we plotted $\Delta G°$ data observed for different Fc model compounds (for compound **9** $\Delta G° = -5.4$ kcal mol^{-1}, while for ferrocenecarboxylic acid $\Delta G° = -4.6$ kcal mol^{-1}).[39]

It is necessary at this point to address a certain number of factors which could affect the value of $F_{\text{pull-off}}$. As already stated above, an intrinsic variability of $F_{\text{pull-off}}$ follows from the probability distribution of $p_{\text{pull-off}}$. Other sources of deviation can be related to differences in the dissociation trajectories of the HG system. Different HG complex geometries could originate from different orientations of the molecular pairs on the two surfaces (tip and substrate) or could be related to the granular structure of the gold layer on the AFM tip as well. However, as stated above for the two integration methods and the theoretical curves reported in Figure 6B, different dissociation pathways probably play a marginal role in determining the $F_{\text{pull-off}}$.

As already addressed above, changes in the integration parameters A_{CD} in eq 4 have been shown to affect only the intercept of the curve of $-\Delta G°$ vs ϵ. This is reflected in the $F_{\text{pull-off}}$ vs $-\Delta G°$ curve determining a $\Delta G°$ interval of ±0.8 kcal mol^{-1}, which is in the same order of magnitude as the experimental error. Furthermore, considering the physical dimensions of the guests and of the β-CD cavity, a value of $r = 2$ Å represents a reasonable approximation that can be applied for all different guests.

Conclusions

Using an atomic force microscope, we determined in aqueous medium the rupture forces of individual HG complexes between β-cyclodextrin SAMs and several surface-confined guests. The analysis of the histograms revealed periodic distributions of forces with loading-rate independent maxima at integer multiples of a certain force quantum characteristic of each guest. The observed force quanta were 39 ± 15, 45 ± 15, 89 ± 15, and 102 ± 15 pN, respectively, and were attributed to the rupture of a single HG complex. These results, in combination with previous reports, indicated that the HG complex rupture forces were probed under thermodynamic equilibrium. Microcalorimetry and SPR measurements were employed to investigate the complex formation for model guest compounds in solution and on β-CD monolayers. The force quanta and the thermodynamic parameters of the inclusion complexes followed the same trend. Finally, a descriptive model based on the evaluation of the energy potential landscape of tip−surface interaction was developed to correlate quantitatively the pull-off force values with $\Delta G°$.

Experimental Section

AFM Tip Modification. Standard V-shaped silicon nitride cantilevers with pyramidal tips (purchased from Digital Instruments (DI), Santa Barbara, CA) were coated with ca. 2 nm of Ti and ca. 50 nm of Au by evaporation in high vacuum at SSENS bv (Hengelo, The Netherlands). The tips were functionalized as described previously[25] in 1 mM ethanolic solutions containing binary mixtures of 2-mercaptoethanol and a guest adsorbate **2**, **3**, **4**, **5**, or **6** (0.2 and 1%), for 16 h at r.t.

(38) This is to monitor multiple times the one datapoint that has a probability p_{contact} significantly different from either 0 or 1, and therefore switching between the "contact" and "out-of-contact" states may be observed.

(39) Godínez, L. A.; Schwartz, L.; Criss, C. M.; Kaifer, A. E. *J. Phys. Chem. B* **1997**, *101*, 3376−3380.

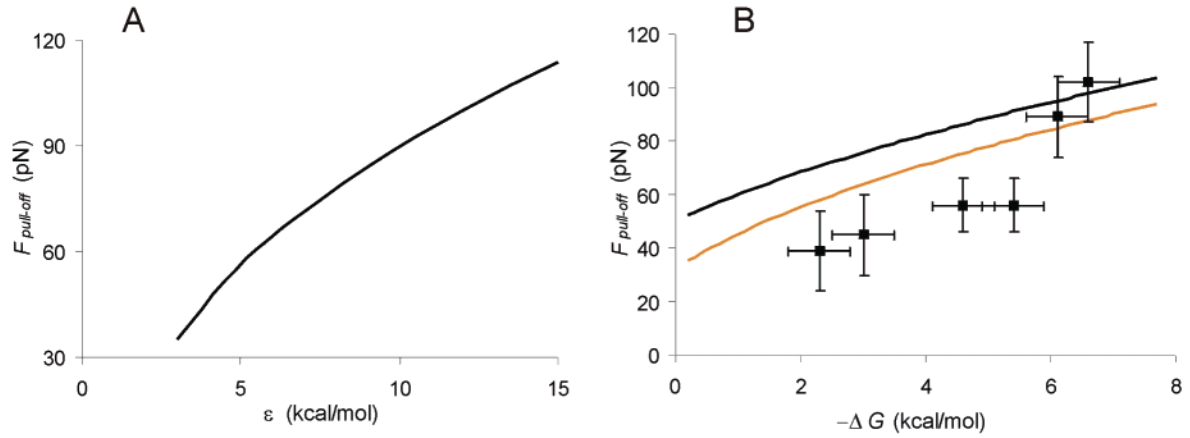

Figure 6. (A) Dependence of $F_{pull-off}$ on ϵ. (B) Experimental pull-off forces vs $-\Delta G°$ (∞) and calculated square root functions for spherical (eq 3) (black solid line) and cylindrical integration (eq 4) (gray solid line). For ferrocene, two $-\Delta G°$ values are reported with the same force value due to different $\Delta G°$ measured for different model compounds (for details, see text).

AFM Measurements and Analysis. The AFM measurements were carried out on a NanoScope III multimode AFM (DI) utilizing a 10 μm (E) scanner and a DI liquid cell on SAMs of **1** on atomically smooth Au(111).[40] The cantilever spring constants k (in the range of 0.05−0.12 N/m) of the gold-coated tips were calibrated using the reference method described by Tortonese and Kirk[41] and by the thermal noise method.[42] Force−displacement (f−d) curves were acquired sequentially in Milli-Q water at different positions on the sample surface. The loading force was kept below 500 pN, and the loading rate was varied between 3.5×10^3 pN/s and 8.8×10^5 pN/s. The quantitative analysis of the observed individual pull-off events was performed as described previously.[25]

Isothermal Titration Calorimetry. Titrations were performed at 25 °C using a Microcal VP-ITC titration microcalorimeter. Sample solutions were prepared using Milli-Q water. Titrations of guests **9**, **10**, and **11** were performed by adding aliquots of a 1 mM β-CD solution to a 0.1 mM guest solution,[28] while 50 mM solutions of compounds **7** and **8** were titrated to β-CD solution 5 mM. The titrations were analyzed using a least squares curve-fitting procedure. Control experiments involved addition of β-CD to water and addition of water to a guest solution.[28]

Surface Plasmon Resonance. SPR measurements were performed in a two-channel vibrating mirror angle scan setup based on the Kretschmann configuration, described by Lenferink et al.[43] Light from a 2 mW HeNe laser was directed onto a prism surface by means of a vibrating mirror. The intensity of the light was measured with a large-area photodiode. This setup allowed determination of changes in plasmon angle with an accuracy of 0.002°. The gold substrate with the monolayer was optically matched to the prism using an index matching oil. A Teflon cell, placed on the monolayer via an O-ring to avoid leakages, was filled with 800 μL of Milli-Q water. After stabilization of the SPR signal, titrations were performed by removing an amount of water and adding the same amount of 0.1 mM stock solution of guest **9**, **10**, or **11**.[28] Between each addition the cell was thoroughly washed with Milli-Q water (700 μL of water 5 times). SPR measurements were repeated 3 times for each monolayer guest system.

Molecular Dynamics. Coordinates for the native β-CD were derived from an X-ray structure, and the water molecules were removed. All calculations were done with Quanta/CHARMm 24.0 and referred to an unsubstituted ferrocene molecule. The cyclodextrin was charged with the charge template method, and excess charge was smoothed over nonpolar carbons and hydrogens. The ferrocene was treated as a rigid body by having large harmonic potentials applied between all carbon−iron pairs. The iron atom had a charge of +2 and the two cyclopentadienyl ligands had a charge of −1. The ferrocene was placed "manually" in the cavity of the cyclodextrin, followed by ABNR minimization until the root-mean square of the energy gradient was ≤0.001 kcal mol^{-1} Å^{-1}. This complex was placed in the center of a cubic box of TIP3P water of 30 Å,[44] as implemented in CHARMm). The ferrocene was translated along the quasi 7-fold axis of the cyclodextrin in steps of 0.5 Å. Overlapping waters were removed (on the basis of heavy-atom interatomic distances of ≤2.3 Å). The positions of the carbon atoms of the cyclodextrin bearing the CH_2OH groups and the Fe were constrained. Before the MD simulations were run, the system was minimized by steepest descent for a maximum of 1000 steps or until a root-mean square of the energy gradient of ≤1 kcal mol^{-1} Å^{-1} was reached. The system was heated to 300 K in 5 ps, followed by equilibration of 10 ps, after which the MD (NVE ensemble, no systematic deviation from 300 K) was run for 100 ps. During the simulation, the nonbonded list was updated every 20 time steps with a cutoff of 14 Å. The van der Waals interactions were treated with a switch function between 10 and 13 Å, whereas the shift function was applied to the electrostatic interactions (cutoff 13 Å). The time step was 1 fs, with the SHAKE algorithm placed on the hydrogens.[45] Coordinate sets were saved regularly and used for subsequent data analysis. The interaction energy between the cyclodextrin and ferrocene was averaged over all data sets.

Acknowledgment. This research has been supported financially by the Council for Chemical Sciences of The Netherlands Organization for Scientific Research (CW-NWO; T.A. Grant No. 97041), the European Union (project Polynano), the Technology Foundation STW, and MESA$^+$ Institute for Nanotechnology.

Supporting Information Available: Full experimental details, XPS data, electrochemistry data for monolayer characterization, MD simulation data and fit to LJP, and derivation of analytical expression of $p_{contact}$ (PDF). This material is available free of charge via the Internet at http://pubs.acs.org.

JA0383569

(40) Schönherr, H.; Vancso, G. J.; Huisman, B.-H.; van Veggel, F. C. J. M.; Reinhoudt, D. N. *Langmuir* **1999**, *15*, 5541−5546.
(41) Tortonese, M.; Kirk, M. *Proc. SPIE* **1997**, *3009*, 53−60.
(42) (a) Hutter, J. L.; Bechhoefer, J. *Rev. Sci. Instrum.* **1993**, *64*, 1868−1873. (b) Sader, J. E. *J. Appl. Phys.* **1998**, *84*, 64−76.
(43) Lenferink, A. T. M.; Kooyman, R. P. H.; Greve, J. *Sens. Actuators, B* **1991**, *3*, 261−265.
(44) Jorgensen, W. L.; Chandrasekhar, J.; Madura, J. D.; Impey, R. W.; Klein, M. L. *J. Chem. Phys.* **1983**, *79*, 926−935.
(45) Berendsen, H. J. C.; Postma, J. P. M.; Dinola, A.; Van Gunsteren, W. F.; Haak, J. R. *J. Chem. Phys.* **1984**, *81*, 3684−3690.